I&EC research
Industrial & Engineering Chemistry Research
pubs.acs.org/IECR
Article

Tandem Hydrodeoxygenation Catalyst System for Hydrocarbons Production from Simulated Bio-oil: Effect of C−C Coupling Catalysts

Isaac Yeboah, Yahao Li, Kishore Rajendran, Kumar R. Rout,* and De Chen*

Cite This: *Ind. Eng. Chem. Res.* 2021, 60, 2136−2143

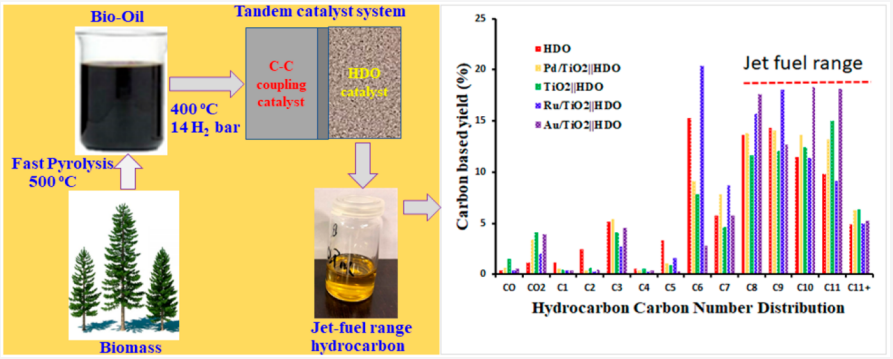

ABSTRACT: Research in the sustainable conversion of biomass to fuels and chemicals is a necessity for the reduction of the carbon footprint in transport energy. Herein, we demonstrate an efficient tandem catalyst to selectively convert (simulated) bio-oil to hydrocarbons with enhanced C_{4+} fuel yield in a fixed bed reactor of a small pilot plant. The tandem catalytic system is a multifunctional dual bed system; carbon coupling catalysts (0.2 wt % X-TiO_2(X: Ru, Pd, Au) at the upper layer and hydrodeoxygenation (Ru-MoFeP/Al_2O_3) at the bottom layer in a single fixed bed reactor. The upper-bed catalysts facilitated the carbon coupling reaction of C_2-C_4 light oxygenates and significantly reduced the light gases yield (C_1-C_5) to ca. 40% and increased the organic (C_{4+}) phase ca. 15%. The analysis of the organic phase suggests that among the screened upstream catalysts, 0.2 wt % Ru/TiO_2||Ru-MoFeP/Al_2O_3 recorded the optimum activity. The coupled light oxygenates (acetone) alkylated with the phenolic compounds and sequentially hydro-deoxygenated to yield higher C_{4+} hydrocarbons. This versatile tandem catalytic approach has a potential application in the emerging biorefinery concept.

1. INTRODUCTION

Lignocellulosic biomass conversion to fuel and chemicals is one of the few options available to reduce the global dependence of fossil fuel for long-distance aviation transport.[1] Woody biomass can be processed through gasification (syngas), pyrolysis (bio-oil), and biochemical pathways while integrating water gas shift, steam reforming, MeOH synthesis, Fischer−Tropsch synthesis (polymerization), hydrodeoxygenation, and zeolite upgrading to yield fungible fuel and chemicals.[2−19]

Fast pyrolysis converts woody biomass to bio-oil, gas, and char.[20] It is of great interest to design catalytic systems to upgrade bio-oil to higher value fuel and biochemicals. Bio-oil has a multifunctional nature and requires a rational design of stable and multifunctional catalysts. Catalytic upgrading of bio-oil to fuel and chemicals has been reviewed by several authors.[11,14,21,22] Hydrodeoxygenation (HDO) and zeolite upgrading to produce hydrocarbons such as aromatics, paraffins, olefins, and coke from waste vegetable oils, algae, lignin, bio-oil, and lignocellulose biomass have been intensively studied.[23−26] In considering bio-oil upgrading, condensed phase bio-oil upgrading and vapor phase upgrading are the main technologies that have been experimentally studied with the common trait of hydrodeoxygenation catalysis.[13,27]

Hydrodeoxygenation of bio-oils occurs at hydro-treating conditions of 300−600 °C in the presence of a heterogeneous catalyst. There have been several reviews about hydrodeoxygenation catalysts, feedstock, and mechanism.[28,11,29−31] The hydrodeoxygenation reaction requires the presence of molecular hydrogen, and thus moderate to high-pressure is required to facilitate reactant covered catalysts and the production of hydrogen.[23] The splitting of molecular hydrogen also requires a metal catalyst to facilitate the dihydrogen dissociation. The dissociated hydrogen (H) aids in the hydrogenation of the C−O bonds in bio-oil. The hydro-

Received: January 10, 2021
Accepted: January 15, 2021
Published: January 26, 2021

https://dx.doi.org/10.1021/acs.iecr.1c00113
Ind. Eng. Chem. Res. 2021, 60, 2136−2143

genation of the C═O bond to C−OH and further dehydration on the acidic sites causes the C−O bond cleavage and water formation. The reaction pathway for multifunctional catalysts has been attributed to a synergistic effect between the metal site (hydrogenation) and the support (metal oxide, Lewis or Brønsted acidity) to yield hydrogenolysis products, hydrocarbon, and water.[32] In this regard, multifunctional catalysts such as Pd/ZrP and Pt/TiO_2 and transition bimetallic phosphide have been applied.[11,22,32,33] The transition bulk bimetallic phosphides (TMP) such as MoP, Fe_2P, Ni_2P, CoP, and WP have been applied in biomass upgrading (HDO reactions) due to their remarkable hydrogen transferability and inherent Lewis acidity.[34−38] The FeMo phosphide catalyst selectively cleaves C−O instead of hydrogenating the aromatic ring followed by subsequent dehydration to produce aromatics instead of cyclic paraffin.[15,38−40] This catalyst has high aromatic selectivity.

However, applying hydrodeoxygenation reaction for pyrolysis vapors leads to undesirable products, light olefins, (C_{4-}). The higher yield of light gas stream (C_1−C_4) products reduces the carbon length in the desired transport fuel range products and increases the minimum selling fuel price (MFSP).[12,41−43] To have biofuel upgraded from bio-oil be cost-competitive with fossil fuel, the C_{4+} yield from the bio-oil should be maximized, and light gas (C_{4-}) yield is minimized.[43] Bio-oil contains about 20% light oxygenates, which ends up in the light gas stream via direct dehydration from the acid sites of the HDO catalyst.[44,45] At moderate temperature conditions, the direct dehydration reaction of light oxygenates could be minimized by introducing catalyzed carbon coupling reactions such as ketonization, aldol condensation, oligomerization, alkylation/alkylation, Diels−Alder, Guerbet, and acylation to yield C−C coupled higher oxygenated products.[46−53] Light oxygenates are very reactive due to the presence of C═O, O−H, and COOH. The acids, carbonyls, and alcohols can undergo carbon chain growth and oxygen removal reactions to high yield C_{5+} oxygenated products. Carbon coupling reactions require using a bifunctional (hydrogenation and dehydration) site. Iglesia et al. used a physically mixed catalyst, Cu/SiO_2 + TiO_2, to study light oxygenates (C_3) coupling to yield longer chain (C_{6+}) oxygenates.[54] The balance between the hydrogenation and Lewis acid−base pair's functionality is reported to be a major contributor to the reducible oxide catalyst design for the carbon coupling reaction.[54] Moreover, Pt/TiO_2 is reported to be active for oxygen removal reactions from bio-oil.[43] However, TiO_2 is also known to catalyzed the aldol condensation reaction.[54] The optimization of hydrogenation sites on the carbon coupling catalyst in tandem with the hydrodeoxygenation catalyst will result in enhanced carbon yield from biomass-derived pyrolysis vapors. Typically, the main challenge has been integrating the carbon coupling reaction and HDO reactions in a single reactor, tuning the acid−base pairs, and optimizing the hydrogenation site, X, in X-TiO_2.

To unravel such a challenge, usually, two reactors are employed.[55] However, a tandem reaction with multifunctional catalysts can circumvent multiple reactors and dehydration of light oxygenates (acids, aldehydes, ketones, alcohol) into smaller olefins. Recently, Tao Zhang studied a tandem catalytic system (dual bed) in a single reactor by integrating Ni/H ‖ CuNi/MgO to convert cellulose to high-density polycycloalkanes.[56]

Here, we demonstrate a versatile tandem, dual bed catalyst system with an upstream catalyst, 0.2 wt %X-TiO_2 (X: Au, Pd, Ru on TiO_2 pellet), and a downstream catalyst of Ru-MoFeP/Al_2O_3 catalysts to effectively convert simulated bio-oil to jet fuel range hydrocarbons with high C_{4+} yield. We focus on the balance of the hydrogenation function (X) and dehydration function in the C−C coupling catalysts and study the effect of C−C coupling catalysts on the activity of the oxygen removal and the product distribution in the tandem catalytic system. The integration of the dual bed catalyst led to the reduction of the light gas yield (C_{4-}) by ca. 40% and increase of biofuel yield (C_{4+}) by ca. 15%, which is crucial to reduce the MFSP of the biofuel.

2. EXPERIMENTAL SECTION

2.1. Materials. All chemicals were used as received from the suppliers: ammonium phosphate dibasic ($(NH_4)_2HPO_4$, Sigma-Aldrich, 99%), iron nitrate nonahydrate ($FeNO_3{\cdot}9H_2O$, Sigma-Aldrich, 99%), ammonium molybdate tetrahydrate ($(NH_4)_6Mo_7O_{24}{\cdot}4H_2O$, Sigma-Aldrich, 99%), $RuCl_3$ (Sigma-Aldrich, 99%), citric acid (Sigma-Aldrich, 99%), and Sasol chemicals USA, LLC, Catalox alumina spheres (surface area, 109.8 m^2/g; size, 4−5.5 mm). Titanium(IV) oxide pellets (surface area, 37 m^2/g; mean pore diameter, 270 Å) were purchased from Thermo Fisher Scientific. Acetic acid, acetol, furfural, phenol, guaiacol, and eugenol were all purchased from Sigma-Aldrich with a purity of greater than 99%.

2.2. Methods: Catalyst Synthesis. Ru-MoFeP/Al_2O_3 was selected as the HDO catalysts based on our previous study,[57] and a detailed study of the HDO catalysts will be reported elsewhere.[57] The present work explores the synthesis of the HDO catalyst for application at relevant industrial conditions in a typical fixed bed reaction. The MoFeP active phase on supported alumina spheres was prepared by a modified Pichini method, using a sequential wetness impregnation method. Aqueous citric acid (0.4 M), an organic chelating agent, was first prepared to create an acidic environment to free the metal salts from precipitating.[58,59] A 1:1:1 molar concentration of Mo/Fe/P was added stepwise onto the 1 M citric acid solution. In the typical experiment in which 100 g of alumina spheres are used, the Mo, Fe, and P precursor weights used are 37.2, 84.8, and 23.9 g, respectively, representing 20 wt % loading of the active metal phase. The light yellowish homogeneous solution formed was impregnated sequentially on the spherical alumina support within a 24 h period. The formed catalyst stayed at room temperature overnight and was dried at 100 °C for 12 h. The catalyst was further calcined in air at a heating rate of 1 °C/min to remain at 350 °C for 6 h. Ru at 1 wt % was then impregnated onto the calcined catalyst using the incipient wetness impregnation method. The Ru-promoted catalyst on MoFeP/Al_2O_3 was subsequently dried 100 °C (4 h) and calcined at 500 °C using 1 °C/min heating rate, to remain at the final temperature for 5 h. The active phase, Ru-MoFeP, was obtained using a temperature-programmed reduction method at a heating rate of 1 °C/min at 250 and 700 °C to react all phosphorus and reduce oxides to the metallic form in the presence of 75% H_2 in nitrogen.[15,38,39] The flow diagram for catalyst synthesis is illustrated in Figure 1.

The synthesis of the X-TiO_2 catalyst was performed using a conventional incipient wetness impregnation method. The precursor solutions (Pt, Ru, Pd, and Au) were prepared in isopropyl alcohol−water mixture (0.2:0.8 vol %). The

https://dx.doi.org/10.1021/acs.iecr.1c00113
Ind. Eng. Chem. Res. 2021, 60, 2136−2143

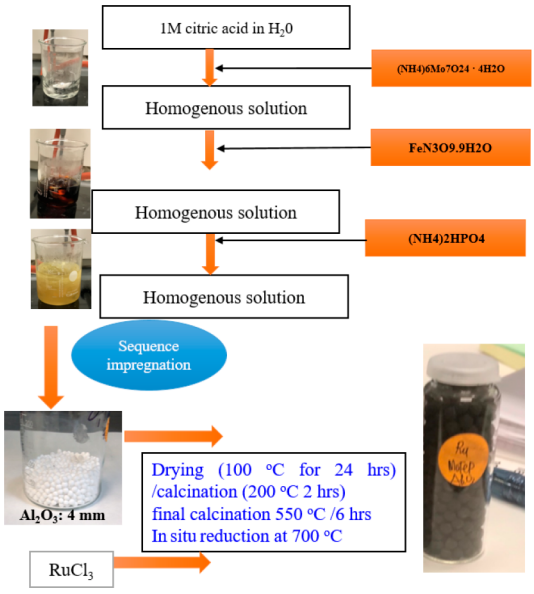

Figure 1. Schematic flow diagram for the synthesis of HDO catalyst.

homogeneous aqueous solution is then impregnated on the support, TiO_2 pellet at room temperature while stirring. The impregnated solution is stored overnight, dried at 100 °C, and calcined (N_2 flow 100 mL/min) at 300 °C, 1 °C/min for 4 h in a furnace.

2.3. Preparation of Simulated Bio-oil. The simulated bio-oil was prepared based on typical wood-derived bio-oil composition obtained by the fast pyrolysis of the lignocellulosic biomass.[60] Distilled water, acetic acid, acetol, furfural, phenol, guaiacol, and eugenol with a weight fraction of 28.7, 12.3, 13.8, 10.6, 15.7, 9.1, and 10.4%, respectively, were weighed into the flask. The prepared feedstock was stored below 5 °C. The acetic acid, acetol, and furfural are typical decomposing products from the hemicellulose fraction of woody biomass, while phenol, guaiacol, and eugenol are monomers derived from lignin. The determined GC-FID chromatogram of the prepared feedstock is shown in Supporting Information, Figure S1. The calculated O/C and H/C ratios were 0.85 and 1.3, respectively, and thus the feed has the resemblance of bio-oil derived from wood.[61]

2.4. Catalyst Characterization. Specific surface area and porosity for the HDO catalyst were examined by N_2 adsorption−desorption isotherms on Micrometrics TriStar 3000 at liquid nitrogen temperature of 77 K. The samples were outgassed in vacuum at 473 K for 12 h before adsorption. The crystal structures of catalysts were identified by powder X-ray diffraction (XRD) measurements (Cu Kα radiation, k = 0.15418 nm, 40 kV, 120 mA) using Bruker D8 Advance. SEM images were taken on the bright-field STEM mode using a Hitachi S-5500 electron microscope operating at an accelerating voltage of 30 kV. The X-ray composition analysis was performed with a JEOL Centurio EDS X-ray spectrometer. The characterization of the HDO catalyst and C−C coupling catalyst can be seen elsewhere.[62,63] Detailed characterization of the synthesized catalyst is reported in section S1. Figures S2, S3, S4, and S5 show the BET isotherms Al_2O_3 spherical support, linear scan of Ru-MoFeP/Al_2O_3 and Au/TiO_2, SEM-EDX mapping of Ru-MoFeP/Al_2O_3, and SEM-EDX mapping of Au/TiO_2, respectively.

2.5. Catalytic Activity Measurement. The tandem reactions were carried out in a mini-pilot plant (fixed bed reactor). A typical pilot plant studies HDO run uses the spherical catalyst Ru-MoFeP/Al_2O_3 for HDO (20 g) and X wt % TiO_2 pellet for ketonization and carbon coupling (20 g), respectively. The HDO reactor is a tubular type with approximate dimensions of 1.0 in. internal diameter (i.d.) 600 mm length. The catalyst was in situ reduced in the total flow rate of 500 mL/min with a 1:1 ratio of N_2 and H_2 for 4 h. The feed mixture (acetic acid, acetol, phenol, guaiacol, eugenol, water, Aldrich, 99.9%) was fed into the reactor by the HPLC pump. The reactant and product concentration were measured by gas chromatography (Agilent 6890) using a phenyl methyl siloxane capillary column (Agilent HP-5, 40 m, 320 μm i.d., 0.25 μm film) connected to an FID and mass spectrometer (MSD 5977 E). An Agilent GC/TCD-FID detector monitored the gas-phase products. The condensed liquid phase product mixture (aqueous and organic phases) were analyzed by a GC-FID (Agilent 6890-5977E) with a mass

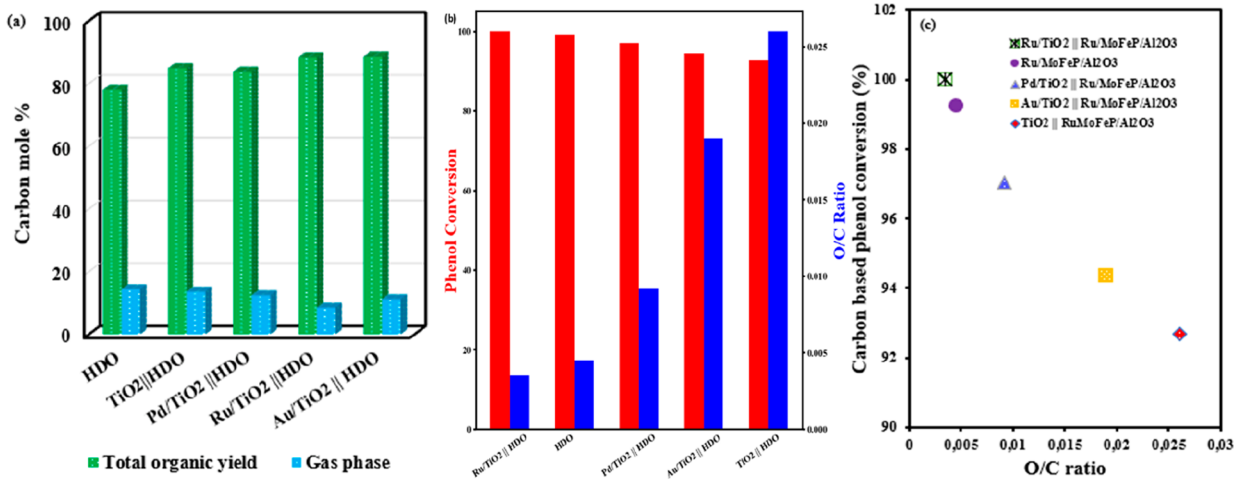

Figure 2. Product fraction obtained from the HDO only and tandem catalytic upgrading of simulated bio-oil to jet-fuel range aromatics: (a) Effects of upstream bed on phenol-based conversion as a function of calculated O/C ratio (b), total pressure 20 bar, H_2 partial pressure 17 bar. Temperature of reaction, 400 °C; reaction time, 6 h; WHSV, excluding water 0.49/h; weight of catalyst, 20 g of HDO (Ru/MoFeP-Al_2O_3) + 20 g of XTiO_2 in the dual bed, and 40 g of HDO (Ru/MoFeP-Al_2O_3) in the single bed.

https://dx.doi.org/10.1021/acs.iecr.1c00113
Ind. Eng. Chem. Res. 2021, 60, 2136−2143

Table 1. Summary of the Carbon-Based Yield of Hydrocarbons on Different Catalysts[a]

carbon mole %	HDO	TiO_2‖HDO	Pd/TiO_2‖HDO	Ru/TiO_2‖HDO	Au/TiO_2‖HDO
gas	14.39	13.64	12.48	8.52	11.23
total organic liquid	78.03	84.89	83.83	88.36	88.59
C4+ (gasoline range hydrocarbons)	77.67	71.67	77.80	88.20	80.40
C7+ (jet-fuel range hydrocarbons)	56.63	60.65	60.80	59.20	71.80
BTX	29.02	20.93	26.32	38.52	19.60
T/B	0.59	0.98	1.64	0.62	2.88
X/B	1.41	2.48	2.91	1.11	5.97

[a]Conditions: total pressure, 20 bar; H_2 partial pressure, 17 bar; temperature of reaction, 400 °C; reaction time, 6 h; WHSV, 0.49/h; weight of catalyst, 20 g of HDO (Ru/MoFeP-Al_2O_3) + 20 g of XTiO_2 in dual bed, and 40 g of HDO (Ru/MoFeP-Al_2O_3) in single bed.

spectrometer detector. Products were identified by NIST11 MS libraries. The peaks with the same molecular weight (Mw) were unified, and their structures were predetermined by GC−MS. Quantitative analysis of the liquid phase products was based on one-dimensional GC-FID analysis (Agilent 7020). Calibration curves for the standard gas and liquid components were used to quantify the composition of hydrocarbons. Equations 1−5 were used in product analysis and quantification.

$$\text{conversion} = \frac{(\text{C, mol, feed}) - (\text{C, mol, reactant})}{\text{C, mol, feed}} \quad (1)$$

$$\text{selectivity} = \frac{\text{C, mol, product, } i}{\sum \text{C, mol, products}} \quad (2)$$

$$\text{DOD \%} = 1 - \frac{\sum \text{oxygen, mol, products}}{\sum \text{carbon, mol, products}} \quad (3)$$

$$\text{O/C} = \frac{\sum \text{oxygen, mol, products}}{\sum \text{carbon, mol, products}} \quad (4)$$

$$\text{carbon, balance} = (\text{C, mass, feed}) - (\text{C, mass, gas}) - (\text{C, mass, char}) - (\text{C, mass, liquid}) \quad (5)$$

3. RESULTS AND DISCUSSION

3.1. Tandem Reaction of C−C Coupling with HDO Catalyst. The catalyst pellets have been characterized by N_2 adsorption and desorption at the liquid N_2 temperature, and SEM-EDS scan. The characterization results are presented in Figures S2−S5, in the Supporting Information. To illustrate the effects of carbon coupling catalysts, the Ru-FeMoP/Al_2O_3 catalyst, the only HDO catalyst, formed after in situ reductions, was initially studied in the mini-pilot plant at the conditions of 1.5 NL/min of H_2 and 0.5 NL/min of N_2 at H_2 partial pressure of 17 bar, 400 °C, WHSV 0.5 h^{-1} with a simulated bio-oil feedstock. Figure 2a illustrates the carbon yields of the organic phase and gas-phase from the pilot plant investigation. The detailed carbon-based yields of the compounds such as the light gas stream (C_1−C_6), BTX, alkylated mononuclear aromatics, and naphthalene in the gas and organic phase are presented in Table S1. The mass balance (wt %) over all the synthesized catalyst and sample GC chromatograms are shown inFigures S6−S8. The carbon balance for both gas and the organic phase is about 92%. A very small amount of acetone and phenol was found in the aqueous phase, and concentration is very low, making accurate quantification difficult. Therefore, the amount of oxygenates that remained in the aqueous phase was not reported here. The results in Table S1 illustrate that Ru-FeMoP/Al_2O_3 is an efficient HDO catalyst and completely converted all the oxygenates in the reactant mixture, except for phenol. It is noted that the condition was selected to focus on the targeted production yield with a high degree of oxygen removal instead of kinetic information. The results in Table S1 are summarized in Table 1. The obtained product yields are much higher than the reported weighted average yield of the liquid organic phase and the gas-phase of 50 and 24 wt %, respectively.[64]

The yield of biofuel (C_{4+}) is 77%, and the yield of the fuel in the jet fuel range (C_{7+}) is 56%. A large amount of polyalkylated aromatics formed on the HDO catalysts (Table 1) suggests that the heavy molecules seem to be formed mostly by the alkylation of aromatics. As discussed above, the higher yield of liquid fuels is always highly desired to reduce the cost of the biofuels.

Tandem reaction was then applied to selectively convert the small molecules to long-chain molecules by C−C bond couplings, such as aldol condensation, ketonization, and aromatic alkylation, to reduce the gas phase yield. It has been shown a duel bed configuration in a single reactor is better than the physical mixture for the C−C coupling during C3 oxygenates (propanal and propanol) conversion. The dual bed catalyst configuration was explored here for the tandem reaction of the mixed oxygenates. The HDO (Ru-MoFeP/Al_2O_3) catalyst was kept unchanged in the second layer, while the TiO_2 and X-TiO_2 (X = Ru, Au, Pd) were used in the first layer for C−C coupling reaction to examine the effects of the upstream catalyst on the overall product distribution. The dual-bed catalysts were defined as (TiO_2 and X-TiO_2: X = Ru, Au, Pd)‖HDO. The noble metals such as Ru, Au, and Pd were used to balance the hydrogenation and C−C coupling functions.

The TiO_2 and the Au, Pd, and Ru impregnated on the TiO_2 pellets were tested at the same reaction conditions while maintaining the space velocity constant based on the total catalyst amount of dual bed catalyst. The ratio of the catalyst amount in two layers was kept constant. The introduction of the C−C coupling catalyst led to a decline in the light gas (Figure 3). The overall carbon balance for the tandem reaction in the duel bed reactor was in a range of more than 96%. The aqueous phase's analysis detected a trace amount of acetone and phenol, and water is dominating in the aqueous phase. Acetone and phenol are the two main remaining oxygen-containing compounds. Acetone is the product of the hydrogenation of acetol and dehydration, and it is also the product of ketonization of acetic acid. Meanwhile, acetone is also a key intermediate for the C−C coupling reaction via aldol condensation on the TiO_2-based catalysts.[63]

https://dx.doi.org/10.1021/acs.iecr.1c00113
Ind. Eng. Chem. Res. 2021, 60, 2136−2143

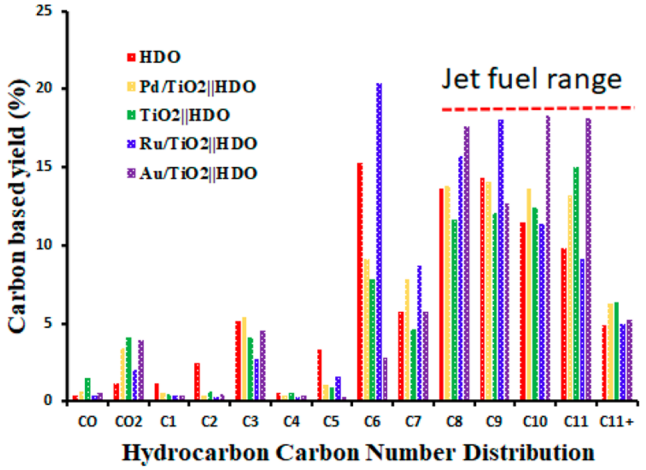

Figure 3. Carbon number distribution in the organic liquid and gaseous product stream derived from HDO only and tandem catalytic upgrading of simulated bio-oil: total pressure, 20 bar; H_2 partial pressure, 17 bar; temperature of reaction, 400 °C.

Phenol is the main oxygen-containing compound that remained from the reactant mixture. The phenol conversion was therefore used to compare the catalysts. Clearly, as seen in Figure 2 panels b and c, the addition of Ru/TiO_2 produced the highest activity in terms of phenol conversion, 100%, and no phenol was observed in the Ru/TiO_2|| $RuMoFeP/Al_2O_3$ experiment, which was found to be better than the neat HDO catalysts. It suggests that Ru/TiO_2 is a better HDO catalyst for phenol conversion than $RuMoFeP/Al_2O_3$. This is consistent with the reported observation that Ru/TiO_2 is highly active for the hydrodeoxygenation of phenolic compounds.[65] Herein, the dual function of Ru/TiO_2 is emphasized, which includes HDO and the C−C coupling reaction in the later discussion. The HDO catalyst alone has a higher phenol conversion than Au/TiO_2, Pd/TiO_2, and TiO_2, which have lower hydrodeoxygenation activity for the phenolic compounds. Also, the O/C ratio in the organic product was further calculated. The calculated elemental O/C ratio for the lowest phenol-based conversion tandem catalysts was 0.025, corresponding to the TiO_2||Ru/MoFeP-Al_2O_3 catalyst. Clearly, in comparing the O/C in the products to the calculated O/C ratio in the feed (0.85), the observed degree of deoxygenation (DOD) was, 99.4, 99.3, 98.8, 97.6, and 97.1% for Ru-TiO_2||Ru-MoFeP/Al_2O_3 > Ru-MoFeP/Al_2O_3 > Pd-TiO_2||Ru-MoFeP/Al_2O_3 > Au-TiO_2||Ru-MoFeP/Al_2O_3 > TiO_2|| RuMoFeP/Al_2O_3, respectively. The yield of biofuels (C_4+) followed the same order and increased from 75.02% (HDO) to 88.2% (Ru-TiO_2||Ru-MoFeP/Al_2O_3). A higher oxygen removal activity was achieved via integrated intramolecular condensation and hydrodeoxygenation reactions.[66]

Furthermore, the overall carbon balance was compared to deduce the total carbon recovered in the gas and organic liquid phase. The TGA analysis of the spent catalyst gave a coke content of less than 2 wt %. In Table 1, the overall carbon recovery for all the tandem reactions was greater than 95%, and higher than the HDO. The gas-phase yield decreased in the dual bed tandem reaction following the order HDO (14.4%) > TiO_2 (13.6%) > Pd-TiO_2 (12.5%) > Au/TiO_2 (11.2%) > Ru-TiO_2 (8.5%), where only the catalysts in the first layer were presented for the dual bed catalysts for clarity reasona. As a result, the total amount of carbon in the organic phase followed the opposite order: HDO (77.7%) < Pd/TiO_2 (83.8%) < TiO_2 (84.9%) < Au/TiO_2 (85.9%) < Ru/TiO_2 (88.4%). The total carbon-based yield in the organic liquid phase was greater than 80% for all the tandem catalyst; thus a higher carbon efficiency was attained.

In addition, Table 1 illustrates the detailed carbon-number yield as a function of the tandem catalysts. Clearly, the CO + CO_2 yield was higher for the Pd/TiO_2||HDO while C_3 (propylene and propane) was also greater for only TiO_2|| HDO. Moreover, the acetone yield observed was higher for Pd/TiO_2||HDO. The increase in CO_2 and acetone possibly suggests that Pd/TiO_2 was the most active catalyst for ketonization of acetic acid to acetone, CO_2, and water. However, in considering the CO_2/CO carbon molar ratio, an indication of the preferred reaction pathway, thus either combined decarboxylation/ketonization (CO_2 release) or decarbonylation (CO release) could be inferred. The CO_2/CO ratio of 6.8, 5.6, 5.5, 3.4, and 2.7 was observed for Au/TiO_2||HDO, Pd/TiO_2||HDO, Ru/TiO_2||HDO, TiO_2, and HDO, respectively. Clearly, decarboxylation and ketonization activity was higher than decarbonylation for these catalysts. The effect of a tandem reaction in dual bed catalysts on the product distribution is presented in Figure 3. A significant dependence of the product distribution on the catalyst configuration was observed. The carbon-based yield of hydrocarbons in the jet fuel range (C_{7+}) increased in the order of HDO (54.0%) < TiO_2 (57.4%) < Ru/TiO_2 (59.2%) < Pd/TiO_2 (60.8%) < Au/TiO_2 (71.8%). The chain growth probability in the C−C coupling reaction can be indicated by the yield of C_{10}−C_{11+}, which follows the order of Ru/TiO_2 < HDO < Pd/TiO_2 < TiO_2 < Au/TiO_2, which follows a similar order of hydrogenation and HDO activity. Only the Ru/TiO_2 catalysts in the dual bed catalysts shifted to light products (higher yield of C_6−C_9 and lower yield of C_{10}−C_{11+}). It can be ascribed by the high hydrogenation activity of Ru. The too-high hydrogenation function terminated the chain growth in the C−C coupling reaction. Other dual bed catalysts have a higher chain growth probability than the HDO catalyst alone. TiO_2 has a low hydrogenation function and thus a higher chain growth probability. However, Au/TiO_2 showed the highest chain growth probability, in which a mild hydrogenation function of Au enhanced aldol condensation reaction occurs.[54,63]

Moreover, the Ru-based upstream catalyst, Ru/TiO_2 gave not only the highest degree of deoxygenation due to the hydrodeoxygenation activity of its highest phenolic compounds, but also the high activity for BTX formation. The lump BTX content decreases in order 38.5, 29.0, 26.3, 20.9, and 19.6 for Ru/TiO_2||HDO, HDO, Pd/TiO_2||HDO, TiO_2|| HDO and Au/TiO_2||HDO, respectively. Possibly, the Ru-promoted upstream catalyst had a higher tendency for the selective formation of BTX, as observed in Table 1. The change in product distribution toward gasoline/jet fuel range hydrocarbons is an indication of the effectiveness of the tandem approach of HDO in a consecutive to C−C coupling catalyst in a single reactor. Besides, it should be noted that the catalyst tolerance of the impurities such as S, Cl, and alkaline metals and long-term stability need to be studied in the future.

In the jet fuel range, the alkylated aromatics are the main compounds on all the catalysts, also on the neat HDO ($RuMoFeP/Al_2O_3$) catalyst as observed from Table S1. It suggests that the HDO catalyst has a high activity of alkylation of aromatics. The possible reactions involved are presented in

https://dx.doi.org/10.1021/acs.iecr.1c00113
Ind. Eng. Chem. Res. 2021, 60, 2136−2143

Figure S9. On the C−C coupling catalysts, hydration, aldol condensation, and ketonization reactions occur. Meanwhile, cyclization and aromatization also occur for alkylated aromatics.[63] In addition, acetone as the intermediate product of the ketonization of the acetic acid, and propanol as the intermediate product of the hydrogenation of acetol, and acetone on the X-TiO_2 catalysts serve as the intermediate agent of the alkylation of aromatics. There is a clear synergy between the two catalyst layers. Propyl-benzene is the richest alkylated aromatics in the jet fuel. Moreover, the yield of propyl-benzene is highest on Ru/TiO_2||HDO. Ru/TiO_2 seems to have high hydrogenation activity leading to a high concentration of intermediates for the alkylation of phenol or aromatics (Table S1).

The observed products once again have a higher value in applications as a gasoline additive or jet-fuel blend fuel. The tandem strategy led to a reduction in gas phase products while increasing the organic liquid yield with much chain growth observed for the Au-impregnated catalyst. The multifunctional feedstock, intermediates, and variable product spectrum suggest that the rational design of a multifunctional catalyst is needed to achieve a higher degree of deoxygenation for the emerging pyrolysis-based biorefinery technology.

4. CONCLUSION

We demonstrated an efficient tandem catalyst system with a dual bed to selectivity convert simulated bio-oil to hydrocarbons with enhanced C_{4+} fuel yield in a fixed bed reactor of a small pilot plant, where carbon coupling catalysts (0.2 wt % X -TiO_2(X: Ru, Pd, Au) and hydro-deoxygenation catalysts (Ru-MoFeP/Al_2O_3) were installed layer by layer in a single reactor. In simulated bio-oil, the most reactive compounds as in bio-oil such as acetic acid, acetol, furfural, phenol, guaiacol, and eugenol were selected. The catalyst pellets were synthesized and characterized. The effects of the hydrogenation function of the metal (X) on the C−C catalysts on the oxygen removal activity and chain-growth probability, and thus the product distribution, were studied. All the dual bed catalysts studied in the present work reduced the formation of light gas yield (C_1−C_5) and enhanced the production of hydrocarbons (C_{7+}) in the jet fuel range. However, the activity of O removal and product distribution depends significantly on the hydrogenation function of metal on TiO_2. The dual bed catalysts 0.2 wt % Ru/TiO_2||Ru-MoFeP/Al_2O_3 showed the best HDO activity, and all the oxygen in the bio-oil, including phenol can be effectively removed at the mild condition with relatively low pressure (20 bar). The system is an effective catalyst for deep O removal. The hydrogenation function of metal on TiO_2 largely influenced the chain growth. Ru has a strong function of hydrogenation, and preferentially terminating the chain growth resulted in a low yield of jet fuel range hydrocarbons but a higher yield of BTX. Au has a mild hydrogenation function and enhanced chain growth leading to a higher yield (71.8%) of jet fuel range hydrocarbons. The coupled light oxygenates (acetone) alkylated with the phenolic compounds and sequentially hydro-deoxygenated to yield higher C_{4+} hydrocarbon. The application of this approach toward vapor phase upgrading of lignocellulosic (biomass) pyrolysis vapors is ongoing and will be reported elsewhere. This versatile tandem catalytic approach has a potential application in the emerging biorefinery concept.

■ ASSOCIATED CONTENT

Supporting Information

The Supporting Information is available free of charge at https://pubs.acs.org/doi/10.1021/acs.iecr.1c00113.

Catalyst characterization and product distribution (PDF)

■ AUTHOR INFORMATION

Corresponding Authors

De Chen − *Department of Chemical Engineering, Norwegian University of Science and Technology, Trondheim 7491, Norway*; orcid.org/0000-0002-5609-5825; Email: de.chen@nt.ntnu.no

Kumar R. Rout − *Department of Chemical Engineering, Norwegian University of Science and Technology, Trondheim 7491, Norway; SINTEF Industry, Trondheim 7491, Norway*; Email: kumarranjan.rout@sintef.no

Authors

Isaac Yeboah − *Department of Chemical Engineering, Norwegian University of Science and Technology, Trondheim 7491, Norway*

Yahao Li − *Department of Chemical Engineering, Norwegian University of Science and Technology, Trondheim 7491, Norway*

Kishore Rajendran − *Department of Chemical Engineering, Norwegian University of Science and Technology, Trondheim 7491, Norway*

Complete contact information is available at: https://pubs.acs.org/10.1021/acs.iecr.1c00113

Notes

The authors declare no competing financial interest.

■ ACKNOWLEDGMENTS

Support from the Research Council of Norway (H_2BioOil and Biomass to Aviation Fuel project in ENERGIX program) and Norwegian University of Science and Technology is highly acknowledged.

■ REFERENCES

(1) Brenes, M. D. *Biomass and bioenergy: new research*; Nova Publishers: 2006.

(2) Sad, M. E.; Neurock, M.; Iglesia, E. Formation of C-C and C-O bonds and oxygen removal in reactions of alkanediols, alkanols, and alkanals on copper catalysts. *J. Am. Chem. Soc.* **2011**, *133* (50), 20384−98.

(3) Ayalur Chattanathan, S.; Adhikari, S.; Abdoulmoumine, N. A review on current status of hydrogen production from bio-oil. *Renewable Sustainable Energy Rev.* **2012**, *16* (5), 2366−2372.

(4) Zhang, H.; Cheng, Y. T.; Vispute, T. P.; Xiao, R.; Huber, G. W. Catalytic conversion of biomass-derived feedstocks into olefins and aromatics with ZSM-5: the hydrogen to carbon effective ratio. *Energy Environ. Sci.* **2011**, *4* (6), 2297−2307.

(5) Jones, A. J.; Iglesia, E. Kinetic, Spectroscopic, and Theoretical Assessment of Associative and Dissociative Methanol Dehydration Routes in Zeolites. *Angew. Chem., Int. Ed.* **2014**, *53*, 12177−12181.

(6) Chang, C. D.; Silvestri, A. J. The conversion of methanol and other O-compounds to hydrocarbons over zeolite catalysts. *J. Catal.* **1977**, *47* (2), 249−259.

(7) Asadieraghi, M.; Daud, W. M. A. W. In-situ catalytic upgrading of biomass pyrolysis vapor: co-feeding with methanol in a multi-zone fixed bed reactor. *Energy Convers. Manage.* **2015**, *92*, 448−458.

(8) Tijmensen, M. J.; Faaij, A. P.; Hamelinck, C. N.; van Hardeveld, M. R. Exploration of the possibilities for production of Fischer−Tropsch liquids and power via biomass gasification. *Biomass Bioenergy* **2002**, *23* (2), 129−152.
(9) Peduzzi, E.; Boissonnet, G.; Haarlemmer, G.; Maréchal, F. Thermo-economic analysis and multi-objective optimization of lignocellulosic biomass conversion to Fischer−Tropsch fuels. *Sustainable Energy and Fuels* **2018**, *2* (5), 1069−1084.
(10) Boerrigter, H.; Den Uil, H.; Calis, H. P. Green diesel from biomass via Fischer−Tropsch synthesis: new insights in gas cleaning and process design. PGBW Expert meeting, Strasbourg, France, October 1, 2002; ECN-RX-03-047; 371−383.
(11) Zacher, A. H.; Olarte, M. V.; Santosa, D. M.; Elliott, D. C.; Jones, S. B. A review and perspective of recent bio-oil hydrotreating research. *Green Chem.* **2014**, *16* (2), 491−515.
(12) Venkatakrishnan, V. K.; Delgass, W. N.; Ribeiro, F. H.; Agrawal, R. Oxygen removal from intact biomass to produce liquid fuel range hydrocarbons via fast-hydropyrolysis and vapor-phase catalytic hydrodeoxygenation. *Green Chem.* **2015**, *17* (1), 178−183.
(13) Venkatakrishnan, V. K.; Degenstein, J. C.; Smeltz, A. D.; Delgass, W. N.; Agrawal, R.; Ribeiro, F. H. High-pressure fast-pyrolysis, fast-hydropyrolysis and catalytic hydrodeoxygenation of cellulose: production of liquid fuel from biomass. *Green Chem.* **2014**, *16* (2), 792−802.
(14) Resende, F. L. Recent advances on fast hydropyrolysis of biomass. *Catal. Today* **2016**, *269*, 148−155.
(15) Rensel, D. J.; Kim, J.; Bonita, Y.; Hicks, J. C. Investigating the multi-functional nature of bimetallic FeMoP catalysts using dehydration and hydrogenolysis reactions. *Appl. Catal., A* **2016**, *524*, 85−93.
(16) Zhao, C.; Camaioni, D. M.; Lercher, J. A. Selective catalytic hydroalkylation and deoxygenation of substituted phenols to bicycloalkanes. *J. Catal.* **2012**, *288*, 92−103.
(17) Taarning, E.; Osmundsen, C. M.; Yang, X.; Voss, B.; Andersen, S. I.; Christensen, C. H. Zeolite-catalyzed biomass conversion to fuels and chemicals. *Energy Environ. Sci.* **2011**, *4* (3), 793−804.
(18) Haniff, M. I.; Dao, L. H. Deoxygenation of carbohydrates and their isopropylidene derivatives over ZSM-5 zeolite catalysts. *Appl. Catal.* **1988**, *39*, 33−47.
(19) Adjaye, J. D.; Bakhshi, N. N. Production of hydrocarbons by catalytic upgrading of a fast pyrolysis bio-oil. Part I: Conversion over various catalysts. *Fuel Process. Technol.* **1995**, *45* (3), 161−183.
(20) Bridgwater, A. V.; Peacocke, G. V. C. Fast pyrolysis processes for biomass. *Renewable Sustainable Energy Rev.* **2000**, *4* (1), 1−73.
(21) Cheng, F.; Brewer, C. E. Producing jet fuel from biomass lignin: Potential pathways to alkyl-benzenes and cycloalkanes. *Renewable Sustainable Energy Rev.* **2017**, *72*, 673−722.
(22) Han, X.; Guo, Y.; Liu, X.; Xia, Q.; Wang, Y. Catalytic conversion of lignocellulosic biomass into hydrocarbons: A mini review. *Catal. Today* **2019**, *319*, 2−13.
(23) Nolte, M. W.; Shanks, B. H. A Perspective on Catalytic Strategies for Deoxygenation in Biomass Pyrolysis. *Energy Technology* **2017**, *5* (1), 7−18.
(24) Wang, C.; Mironenko, A. V.; Raizada, A.; Chen, T.; Mao, X.; Padmanabhan, A.; Vlachos, D. G.; Gorte, R. J.; Vohs, J. M. Mechanistic Study of the Direct Hydrodeoxygenation of m-Cresol over WOx-Decorated Pt/C Catalysts. *ACS Catal.* **2018**, *8*, 7749−7759.
(25) Lin, F.; Zhang, J.; Liu, D.; Chin, Y. H. Cascade Reactions in Tunable Lamellar Micro- and Mesopores for C = C Bond Coupling and Hydrocarbon Synthesis. *Angew. Chem., Int. Ed.* **2018**, *57* (39), 12886−12890.
(26) Huber, G. W.; Corma, A. Synergies between Bio- and Oil Refineries for the Production of Fuels from Biomass. *Angew. Chem., Int. Ed.* **2007**, *46* (38), 7184−7201.
(27) Marker, T. L.; Felix, L. G.; Linck, M. B.; Roberts, M. J. Integrated hydropyrolysis and hydroconversion (IH2) for the direct production of gasoline and diesel fuels or blending components from biomass, part 1: Proof of principle testing. *Environ. Prog. Sustainable Energy* **2012**, *31* (2), 191−199.
(28) Furimsky, E. Catalytic hydrodeoxygenation. *Appl. Catal., A* **2000**, *199* (2), 147−190.
(29) Si, Z.; Zhang, X.; Wang, C.; Ma, L.; Dong, R. An Overview on Catalytic Hydrodeoxygenation of Pyrolysis Oil and Its Model Compounds. *Catalysts* **2017**, *7* (6), 169.
(30) Saidi, M.; Samimi, F.; Karimipourfard, D.; Nimmanwudipong, T.; Gates, B. C.; Rahimpour, M. R. Upgrading of lignin-derived bio-oils by catalytic hydrodeoxygenation. *Energy Environ. Sci.* **2014**, *7* (1), 103−129.
(31) Robinson, A. M.; Hensley, J. E.; Medlin, J. W. Bifunctional Catalysts for Upgrading of Biomass-Derived Oxygenates: A Review. *ACS Catal.* **2016**, *6* (8), 5026−5043.
(32) Griffin, M. B.; Ferguson, G. A.; Ruddy, D. A.; Biddy, M. J.; Beckham, G. T.; Schaidle, J. A. Role of the Support and Reaction Conditions on the Vapor-Phase Deoxygenation of m-Cresol over Pt/C and Pt/TiO2 Catalysts. *ACS Catal.* **2016**, *6* (4), 2715−2727.
(33) Zhou, G.; Jensen, P. A.; Le, D. M.; Knudsen, N. O.; Jensen, A. D. Atmospheric Hydrodeoxygenation of Biomass Fast Pyrolysis Vapor by MoO3. *ACS Sustainable Chem. Eng.* **2016**, *4* (10), 5432−5440.
(34) Whiffen, V. M.L.; Smith, K. J.; Straus, S. K. The influence of citric acid on the synthesis and activity of high surface area MoP for the hydrodeoxygenation of 4-methylphenol. *Appl. Catal., A* **2012**, *419*, 111−125.
(35) Zhao, H. Y.; Li, D.; Bui, P.; Oyama, S. T. Hydrodeoxygenation of guaiacol as model compound for pyrolysis oil on transition metal phosphide hydroprocessing catalysts. *Appl. Catal., A* **2011**, *391* (1−2), 305−310.
(36) Li, K.; Wang, R.; Chen, J. Hydrodeoxygenation of anisole over silica-supported Ni2P, MoP, and NiMoP catalysts. *Energy Fuels* **2011**, *25* (3), 854−863.
(37) Infantes-Molina, A.; Gralberg, E.; Cecilia, J. A.; Finocchio, E.; Rodríguez-Castellón, E. Nickel and cobalt phosphides as effective catalysts for oxygen removal of dibenzofuran: role of contact time, hydrogen pressure and hydrogen/feed molar ratio. *Catal. Sci. Technol.* **2015**, *5* (6), 3403−3415.
(38) Rensel, D. J.; Rouvimov, S.; Gin, M. E.; Hicks, J. C. Highly selective bimetallic FeMoP catalyst for C-O bond cleavage of aryl ethers. *J. Catal.* **2013**, *305*, 256−263.
(39) Rensel, D. J.; Kim, J.; Jain, V.; Bonita, Y.; Rai, N.; Hicks, J. C. Composition-directed FeXMo2-XP bimetallic catalysts for hydrodeoxygenation reactions. *Catal. Sci. Technol.* **2017**, *7* (9), 1857−1867.
(40) Bonita, Y.; Hicks, J. C. Periodic Trends from Metal Substitution in Bimetallic Mo-Based Phosphides for Hydrodeoxygenation and Hydrogenation Reactions. *J. Phys. Chem. C* **2018**, *122* (25), 13322−13332.
(41) Marker, T. L.; Felix, L. G.; Linck, M. B.; Roberts, M. J.; Ortiz-Toral, P.; Wangerow, J. Integrated hydropyrolysis and hydroconversion (IH2®) for the direct production of gasoline and diesel fuels or blending components from biomass, Part 2: continuous testing. *Environ. Prog. Sustainable Energy* **2014**, *33* (3), 762−768.
(42) Venkatakrishnan, V. K.; Delgass, W. N.; Ribeiro, F. H.; Agrawal, R. Oxygen removal from intact biomass to produce liquid fuel range hydrocarbons via fast-hydropyrolysis and vapor-phase catalytic hydrodeoxygenation. *Green Chem.* **2015**, *17*, 178−183.
(43) Griffin, M. B.; Iisa, K.; Wang, H.; Dutta, A.; Orton, K. A.; French, R. J.; Santosa, D. M.; Wilson, N.; Christensen, E.; Nash, C.; Van Allsburg, K. M.; Baddour, F. G.; Ruddy, D. A.; Tan, E. C. D.; Cai, H.; Mukarakate, C.; Schaidle, J. A. Driving towards cost-competitive biofuels through catalytic fast pyrolysis by rethinking catalyst selection and reactor configuration. *Energy Environ. Sci.* **2018**, *11* (10), 2904−2918.
(44) Routray, K.; Barnett, K. J.; Huber, G. W. Hydrodeoxygenation of Pyrolysis Oils. *Energy Technology* **2017**, *5* (1), 80−93.
(45) Prasomsri, T.; Nimmanwudipong, T.; Román-Leshkov, Y. Effective hydrodeoxygenation of biomass-derived oxygenates into unsaturated hydrocarbons by MoO3 using low H2 pressures. *Energy Environ. Sci.* **2013**, *6* (6), 1732−1738.

https://dx.doi.org/10.1021/acs.iecr.1c00113
Ind. Eng. Chem. Res. 2021, 60, 2136−2143

(46) Sutton, A. D.; Waldie, F. D.; Wu, R.; Schlaf, M.; Louis, A.; Gordon, J. C. The hydrodeoxygenation of bioderived furans into alkanes. *Nat. Chem.* **2013**, *5*, 428.
(47) Du, J.; Say, R. F.; Lü, W.; Fuchs, G.; Einsle, O. Active-site remodelling in the bifunctional fructose-1,6-bisphosphate aldolase/phosphatase. *Nature* **2011**, *478*, 534.
(48) Xia, Q. N.; Cuan, Q.; Liu, X. H.; Gong, X. Q.; Lu, G. Z.; Wang, Y. Q. Pd/NbOPO4 multi-functional catalyst for the direct production of liquid alkanes from aldol adducts of furans. *Angew. Chem., Int. Ed.* **2014**, *53* (37), 9755−9760.
(49) Gollwitzer, A.; Dietel, T.; Kretschmer, W. P.; Kempe, R. A broadly tunable synthesis of linear α-olefins. *Nat. Commun.* **2017**, *8* (1), 1226.
(50) Mo, F.; Dong, G. Regioselective ketone α-alkylation with simple olefins via dual activation. *Science* **2014**, *345* (6192), 68−72.
(51) Ose, T.; Watanabe, K.; Mie, T.; Honma, M.; Watanabe, H.; Yao, M.; Oikawa, H.; Tanaka, I. Insight into a natural Diels-Alder reaction from the structure of macrophomate synthase. *Nature* **2003**, *422*, 185.
(52) Anbarasan, P.; Baer, Z. C.; Sreekumar, S.; Gross, E.; Binder, J. B.; Blanch, H. W.; Clark, D. S.; Toste, F. D. Integration of chemical catalysis with extractive fermentation to produce fuels. *Nature* **2012**, *491*, 235.
(53) Climent, M. J.; Corma, A.; Iborra, S. Conversion of biomass platform molecules into fuel additives and liquid hydrocarbon fuels. *Green Chem.* **2014**, *16* (2), 516−547.
(54) Wang, S.; Goulas, K.; Iglesia, E. Condensation and esterification reactions of alkanals, alkanones, and alkanols on TiO2: Elementary steps, site requirements, and synergistic effects of bifunctional strategies. *J. Catal.* **2016**, *340*, 302−320.
(55) Gurbuz, E. I.; Kunkes, E. L.; Dumesic, J. A. Dual-bed catalyst system for C-C coupling of biomass-derived oxygenated hydrocarbons to fuel-grade compounds. *Green Chem.* **2010**, *12* (2), 223−227.
(56) Liu, Y.; Li, G.; Hu, Y.; Wang, A.; Lu, F.; Zou, J. J.; Cong, Y.; Li, N.; Zhang, T. Integrated Conversion of Cellulose to High-Density Aviation Fuel. *Joule* **2019**, *3* (4), 1028−1036.
(57) Yeboah, I. *Tandem Catalytic upgrading of biomass fast-pyrolysis constituents to fuels*. Ph.D. Thesis, Norwegian University of Science and Technology, Norway, 2019.
(58) Zhao, T.; Boullosa-Eiras, S.; Yu, Y.; Chen, D.; Holmen, A.; Ronning, M. Synthesis of Supported Catalysts by Impregnation and Calcination of Low-Temperature Polymerizable Metal-Complexes. *Top. Catal.* **2011**, *54* (16), 1163.
(59) Boullosa-Eiras, S.; Zhao, T.; Chen, D.; Holmen, A. Effect of the preparation methods and alumina nanoparticles on the catalytic performance of Rh/ZrxCe1-xO2-Al2O3 in methane partial oxidation. *Catal. Today* **2011**, *171* (1), 104−115.
(60) Gao, N.; Li, A.; Quan, C.; Du, L.; Duan, Y. TG-FTIR and Py-GC/MS analysis on pyrolysis and combustion of pine sawdust. *J. Anal. Appl. Pyrolysis* **2013**, *100*, 26−32.
(61) Mohan, D.; Pittman, C. U., Jr; Steele, P. H. Pyrolysis of wood/biomass for bio-oil: a critical review. *Energy Fuels* **2006**, *20* (3), 848−889.
(62) Yeboah, I.; Feng, X.; Wenzhao, F.; Mawanga, M.; Rout, K. R.; Duan, X.; Zhou, X.; Chen, D. Ru Induced Multi-functional Catalyst for Jet Fuel Range Hydrocarbon Production from Simulated Bio-oil. *ACS Catal.* **2021**.
(63) Yeboah, I.; Feng, X.; Wang, G.; Rout, K. R.; Cai, Z.; Duan, X.; Zhou, X.; Chen, D. Jet Fuel Range Hydrocarbon Production from Propanal: Mechanistic Insights into Active Site Requirement of a Dual-Bed Catalyst. *ACS Sustainable Chem. Eng.* **2020**, *8* (25), 9434−9446.
(64) Stummann, M. Z.; Høj, M.; Schandel, C. B.; Hansen, A. B.; Wiwel, P.; Gabrielsen, J.; Jensen, P. A.; Jensen, A. D. Hydrogen assisted catalytic biomass pyrolysis. Effect of temperature and pressure. *Biomass Bioenergy* **2018**, *115*, 97−107.
(65) Wan, S.; Pham, T.; Zhang, S.; Lobban, L.; Resasco, D.; Mallinson, R. Direct catalytic upgrading of biomass pyrolysis vapors by a dual function Ru/TiO2 catalyst. *AIChE J.* **2013**, *59* (7), 2275−2285.
(66) Kubička, D.; Horáček, J.; Setnička, M.; Bulánek, R.; Zukal, A.; Kubičková, I. Effect of support-active phase interactions on the catalyst activity and selectivity in deoxygenation of triglycerides. *Appl. Catal., B* **2014**, *145*, 101−107.

https://dx.doi.org/10.1021/acs.iecr.1c00113
Ind. Eng. Chem. Res. 2021, 60, 2136−2143